

# Diffusion of Ga adatoms at the surface of GaAs(001) $c(4 \times 4)$ $\alpha$ and $\beta$ reconstructions.

Marcin Mińkowski <sup>†</sup> and Magdalena A Załuska-Kotur <sup>†,‡</sup>

<sup>†</sup>*Institute of Physics, Polish Academy of Sciences, Al. Lotników 32/46, 02-668 Warsaw, Poland*

<sup>‡</sup>*Faculty of Mathematics and Natural Sciences, Card. Stefan Wyszyński University, ul Dewajtis 5, 01-815 Warsaw, Poland \**  
(Dated: November 13, 2014)

Diffusion of Ga adatom at the As rich, low temperature  $c(4 \times 4)$  reconstructions of GaAs(001) surface is analyzed. We use known energy landscape for the motion of Ga adatom at two different  $\alpha$  and  $\beta$  surface phases to calculate diffusion tensor by means of the variational approach. Diffusion coefficient describes the character of low density adatom system motion at the surface. The resulting expressions allow to identify main paths of an adatom diffusion and to calculate an activation energy of this process. It is shown that diffusion at the  $\alpha$  surface is slower and more anisotropic than this for the  $\beta$  surface.

PACS numbers: 02.50.Ga, 66.10.Cb, 66.30.Pa, 68.43.Jk

## I. INTRODUCTION

Surface diffusion is a control factor of layer by layer crystal growth, the one of basic processes in the construction of nanotechnological devices. The analysis of surface diffusion is based on the determination of adsorption sites, adparticle binding energy at each of these sites and barriers for thermally activated jumps between them. When all these parameters are calculated, the next step is to describe particle diffusion process in this energy landscape. Development of ab-initio calculations in the last years resulted in very accurate description of the surface energy landscape at various systems<sup>1-14</sup>. For many crystals, important because of their applications in nanotechnology or biotechnology, full energy map at the specific surface orientations and reconstructions were done. The system which is often a subject of study is the surface GaAs(001) in its various phases such as high temperature  $(2 \times 4)$ <sup>15,16</sup> or low temperature  $c(4 \times 4)$ <sup>16-27</sup> reconstructions. This semiconductor is very important in production of solar cells or microwave circuits used in cellular phones. In this study we use presented in Refs. 1 and 2 results of ab-initio calculations of energy landscape of As rich  $c(4 \times 4)\beta$  and  $c(4 \times 4)\alpha$  phases for Ga adatom. On the base of these data we derive diffusion coefficient for Ga atoms and compare diffusive motion at both surface structures.

The first observations at low temperatures and at the excess of As atoms established the existence of  $c(4 \times 4)\beta$  structure<sup>17-21</sup> and then asymmetric phase  $c(4 \times 4)\alpha$ <sup>20-27</sup> was found. It is generally accepted now that As-rich  $c(4 \times 4)$  surface is divided into two phases: the  $c(4 \times 4)\alpha$  phase (terminated by Ga - As dimers) which depending on the As pressure exists up to 400- 550 K and the  $c(4 \times 4)\beta$  phase (terminated by As - As dimers) between 400K and 770K<sup>16,20</sup>. Incorporation and then diffusion of Ga atoms control growth process in As rich conditions. That is why detailed knowledge of the Ga adatoms diffusion is so important. Derivation of binding energies and diffusion barriers is the first step in such study. Further analysis can be based on some qualitative analysis of the energy structure<sup>1,2</sup>, Monte Carlo simulation data<sup>20,28-30</sup>

or derivation of analytic formulas<sup>15,30,31</sup>.

The analytic formulas have this advantage over other methods that they give results as a function of temperature and of all other model parameters. We propose new, variational approach, that was first shown to work for many-particle diffusion process<sup>32-36</sup>. Below we show how the variational approach can be used in calculation of tracer diffusion coefficient, which describes also diffusion in the system of low density. For systems of low density correlations can be neglected. However the analysis of adatom motion is still not easy because the reconstructed surface of GaAs(001) $c(4 \times 4)$  in both  $\alpha$  and  $\beta$  versions contain many adsorption sites for Ga adatoms and complicated lattice of possible jumps between them. Calculation of an effective diffusion coefficients in different directions and the analysis of possible modes of particle motion is very difficult when adatom diffuses over the surface of complex energy landscape. It appears that on using proper variational analysis we end up with one formula for diffusion tensor, which then can be analyzed further. Presented approach allows for systematic study of the diffusive particle motion over the surface with definite pattern of energies of adatom at lattice sites and energy barriers for jumps between them.

Below we present the general method of calculations, then we show how it works in the case of GaAs(001) surface in two different  $c(4 \times 4)\beta$  and  $c(4 \times 4)\alpha$  reconstructions of the surface. We show that diffusion decreases and becomes more anisotropic when  $\beta$  reconstruction of the surface changes to  $\alpha$  type. The final expressions for the diffusion coefficient allow to identify main diffusion paths in all cases. Effective activation energy value can be calculated for the diffusion coefficient and for each diffusion path separately.

## II. CALCULATION OF THE DIFFUSION COEFFICIENT.

To describe random walk of single or uncorrelated adatoms over crystal surface we define the tracer diffu-

sion tensor<sup>31,37</sup>

$$D_{n,m} = \lim_{t \rightarrow \infty} \frac{1}{4t} \langle \Delta r_n(t) \Delta r_m(t) \rangle \quad (1)$$

where  $\Delta r_{n[m]}(t)$  is the adsorbate displacement after time  $t$  with respect to the initial position, along the coordinate  $n[m] = x, y$ . Definition (1) in experimental situation corresponds to diffusion coefficient for the adatom system of low density. Adatom diffusion which we want to describe realizes in random walk motion between different adsorption sites located at the crystal surface. To analyze this motion let us divide the lattice of adsorption sites at crystal surface into unit cells. We assume that each cell contains  $m$  sites located in positions  $\vec{r}_j^\alpha = \vec{r}_j + \vec{a}_\alpha$ ;  $\alpha = 1, \dots, m$ , where  $\vec{r}_j$  describes given cell location and  $\vec{a}_\alpha$  is a location of the site within the cell. Particle at the site described by parameters  $(j, \alpha)$  has an energy  $E_\alpha$ . The equilibrium probability of finding adatom at this site is equal to  $P_{eq}(\alpha) = \rho \exp[-\beta E(\alpha)] / \sum_\gamma \exp[-\beta E(\gamma)]$ , where sum is over all sites in the unit cell,  $\beta = 1/(k_B T)$  means inverse temperature parameter and  $\rho$  is density of particles at the surface calculated as number of particles divided by number of unit cells.

The diffusion motion consists of a series of thermally activated jumps. The adsorbate in an initial adsorption state  $\alpha$  after a given time escapes to another adsorption site  $\gamma$  with a transition probability per unit time  $W(j, \alpha; l, \gamma)$ . In order to determine the transition probabilities, we apply the transition state theory<sup>38</sup>, according to which  $W(j, \alpha; l, \gamma)$  are functions of the difference between energy barrier  $\tilde{E}(j, \alpha; l, \gamma)$  for particle jump between sites  $j, \alpha$  and  $l, \gamma$  and  $E(\alpha)$ , the particle energy at the initial adsorption site

$$W(j, \alpha; l, \gamma) = W_{\alpha, \gamma} = \exp\{-\beta[\tilde{E}(j, \alpha; l, \gamma) - E(\alpha)]\}. \quad (2)$$

Both energies can be derived from ab-initio calculations<sup>1,29,39</sup>. Note that particle can jump within one cell or between two different cells  $j$  and  $l$ , so energy  $\tilde{E}$  depends on parameters  $j, \alpha; l, \gamma$  where  $l = j$  when both sites belong to the same elementary cell or  $j \neq l$  when particle changes cell on jumping.  $E(\alpha)$  depends only on the type  $\alpha$  of the site within given cell. The structure of all possible transitions at the surface can be quite complex, especially when they happen between sites of different energy located irregularly within the cell.

Diffusion coefficient defined by (1) refers to single particle motion and we assume that our low density system is a collection of independently moving single particles. The probability that the particle occupies given site changes with time according to the classical Master equation

$$\frac{d}{dt} P(j, \alpha; t) = \sum_{l, \gamma} [W_{\gamma, \alpha} P(l, \gamma; t) - W_{\alpha, \gamma} P(j, \alpha; t)] \quad (3)$$

where  $W_{\gamma, \alpha}$  describe rates of all possible adatom jumps over the lattice and fulfill detailed balance condition

$$W_{\gamma, \alpha} P_{eq}(\gamma) = W_{\alpha, \gamma} P_{eq}(\alpha). \quad (4)$$

All components  $W$  can be gathered in one matrix  $\hat{W}$  with elements  $-\sum_{l, \gamma} W_{\alpha, \gamma}$  at the diagonal location  $(j, \alpha; j, \alpha)$  and  $W_{\gamma, \alpha}$  out of the diagonal.

In order to analyze the character of particle diffusion it is convenient to make Fourier transform of the Master equation (3) basing on the fact that infinite surface over which the particle is wandering consists of periodically repeated cells. In the wavevector  $\vec{k}$  space the vector describing probability of the site occupation has components  $P_\alpha(\vec{k}; t) = \sum_j \exp(i\vec{k}\vec{r}_j^\alpha) P(j, \alpha; t)$ . Each component  $\alpha$  of this vector corresponds to one of the sites within unit cell. We have now  $m$  equations for  $m$  different components of the occupation probability vector

$$\frac{d}{dt} P_\alpha(\vec{k}; t) = \sum_{\gamma \neq \alpha} M(\gamma; \alpha) P_\gamma(\vec{k}; t) + M(\alpha; \alpha) P_\alpha(\vec{k}; t). \quad (5)$$

Matrix  $\hat{M}$  is created from matrix  $\hat{W}$  after transformation into  $k$  space what gives

$$\begin{aligned} M(\alpha, \alpha) &= - \sum_{l, \gamma \neq \alpha} W_{\alpha, \gamma} \\ M(\gamma, \alpha) &= W_{\gamma, \alpha} e^{i\vec{k}(\vec{r}_l^\gamma - \vec{r}_j^\alpha)} \end{aligned} \quad (6)$$

where formulas are written for one, arbitrary cell  $j$  and summation goes over all sites within this cell and over all neighboring cells  $l$ . Note that off-diagonal elements  $M(\gamma, \alpha)$  are  $\vec{k}$  dependent.

To solve set of equations (5) we should find  $m$  eigenvalues and eigenvectors of matrix  $\hat{M}$ . Each eigenvalue describes one dynamical mode responsible for the relaxation of the initial occupation probability towards equilibrium values. The diffusion tensor (1) can be obtained from the one particular eigenvalue of the transition rate matrix (6). It can be demonstrated<sup>31,32,40</sup> that for the master equation (5) there is one and only one eigenvalue  $\lambda_D(\vec{k})$  such that  $\lim_{\vec{k} \rightarrow 0} \lambda_D(\vec{k}) = 0$  and the real part of all the other eigenvalues is negative. This particular eigenvalue  $\lambda_D$  is diffusional eigenvalue, what means that it is proportional to  $\vec{k}^2$  and can be expressed as

$$\lim_{\vec{k} \rightarrow 0} \lambda_D = \lim_{\vec{k} \rightarrow 0} \frac{\vec{w} \hat{M} \vec{v}}{\vec{w} \vec{v}} = -\vec{k} \hat{D} \vec{k} \quad (7)$$

Where  $\vec{w}$  is the left eigenvector and  $\vec{v}$  the right one. The matrix  $\hat{M}$  is not hermitian but its elements are related to each other by the rule  $M^*(\gamma; \alpha) P_{eq}(\gamma) = M(\alpha; \gamma) P_{eq}(\alpha)$  resulting from the local equilibrium balance (4). As a result eigenvectors of matrix  $\hat{M}$  are connected by relation  $w_\alpha^* P_{eq}(\alpha) = v_\alpha$ . Equation (7) is our main formula used to derive diffusion matrix  $\hat{D}$  (1). On inserting explicit expressions (6) into (7) and taking into account normalization

$$\sum_\alpha w_\alpha v_\alpha = \sum_\alpha w_\alpha w_\alpha^* P_{eq}(\alpha) = \rho \quad (8)$$

we can write

$$\begin{aligned}\vec{k}\hat{D}\vec{k} &= \frac{1}{\rho} \lim_{\vec{k} \rightarrow 0} \sum_{\alpha, \gamma} w_{\gamma} M(\alpha, \gamma) v_{\alpha} \\ &= \frac{1}{\rho} \lim_{\vec{k} \rightarrow 0} \sum_{\alpha, \gamma} (w_{\alpha} - e^{\vec{k}(\vec{r}_i^{\gamma} - \vec{r}_j^{\alpha})} w_{\gamma}) W_{\alpha, \gamma} v_{\alpha}.\end{aligned}\quad (9)$$

And when consequences of detailed balance for  $M(\alpha, \gamma)$  and eigenvectors  $\vec{w}, \vec{v}$  are taken into account we have

$$\begin{aligned}\vec{k}\hat{D}\vec{k} &= \frac{1}{\rho} \lim_{\vec{k} \rightarrow 0} \left[ \sum_{\alpha > \gamma} (w_{\alpha} - e^{\vec{k}(\vec{r}_i^{\gamma} - \vec{r}_j^{\alpha})} w_{\gamma}) W_{\alpha, \gamma} P_{eq}(\alpha) w_{\alpha}^* \right. \\ &\quad \left. + (e^{\vec{k}(\vec{r}_i^{\gamma} - \vec{r}_j^{\alpha})} w_{\gamma} - w_{\alpha}) W_{\alpha, \gamma} P_{eq}(\alpha) w_{\gamma}^* e^{-\vec{k}(\vec{r}_i^{\gamma} - \vec{r}_j^{\alpha})} \right] \\ &= \frac{1}{\rho} \lim_{\vec{k} \rightarrow 0} \sum_{\alpha > \gamma} |w_{\alpha} - e^{\vec{k}(\vec{r}_i^{\gamma} - \vec{r}_j^{\alpha})} w_{\gamma}|^2 W_{\alpha, \gamma} P_{eq}(\alpha) \quad (10)\end{aligned}$$

Our diffusional eigenvalue  $\lambda_D$  in the limit of small  $\vec{k}$  is proportional to  $\vec{k}^2$  and has the lowest absolute value of all eigenvalues. It can be found by the variational method on assuming properly parameterized eigenvector. We choose

$$\begin{aligned}v_{\alpha} &= P_{eq}(\alpha) e^{i\vec{k}\vec{\phi}_{\alpha}} \\ w_{\alpha} &= e^{-i\vec{k}\vec{\phi}_{\alpha}}\end{aligned}\quad (11)$$

The above form of eigenvectors provides proper normalization and introduces variational parameters  $\vec{\phi}_{\alpha}$  that are coupled to wave-vector  $\vec{k}$  so they can influence diffusion coefficient. Similar choice of variational parameters was shown to be a good one in description of collective diffusion at non-homogeneous surfaces in Refs. 33–36.

On using explicit expression for eigenvectors (11) in the last equation (10) we obtain variational formula for diffusion coefficient  $\hat{D}_{var}$

$$\begin{aligned}\vec{k}\hat{D}_{var}\vec{k} &= \lim_{\vec{k} \rightarrow 0} \sum_{\alpha > \gamma} W(\alpha; \gamma) P_{eq}(\alpha) [e^{i\vec{k}\vec{\phi}_{\alpha}} - e^{\vec{k}(\vec{r}_i^{\gamma} - \vec{r}_j^{\alpha}) + \vec{\phi}_{\gamma}}]^2 \\ &= \sum_{\alpha > \gamma} W(\alpha; \gamma) P_{eq}(\alpha) [\vec{k}(\vec{\phi}_{\gamma} + \vec{r}_i^{\gamma} - \vec{r}_j^{\alpha} - \vec{\phi}_{\alpha})]^2 \quad (12)\end{aligned}$$

Now, for the final expression for  $\hat{D}_{var}$  we should minimize the above equation with respect to all independent parameters  $\vec{\phi}_{\alpha}$ . Each separate type of the surface site  $\alpha$  has its individual vector of phases, so all together we have two times more phases than sites in the elementary cage. However one of vector parameters  $\vec{\phi}$  can be set to be  $\vec{0}$ , because as it can be seen in (12) only phase differences count, what means that we can move all phases by the same quantity without changing the result. Moreover phases for some sites are identical due to the system symmetry. In such a way the number of parameters can be reduced and as a result the problem is simplified. In the following sections we will show how the procedure works in practice on studying diffusion of Ga adatoms over GaAs(001)  $c(4 \times 4)$  surface.

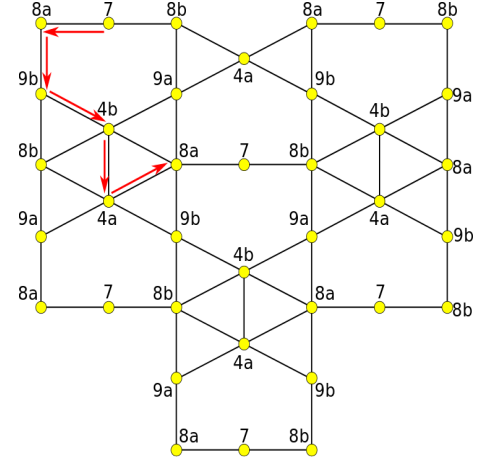


FIG. 1: Binding sites of Ga atoms at the GaAs(001)- $c(4 \times 4)$   $\beta$  surface.

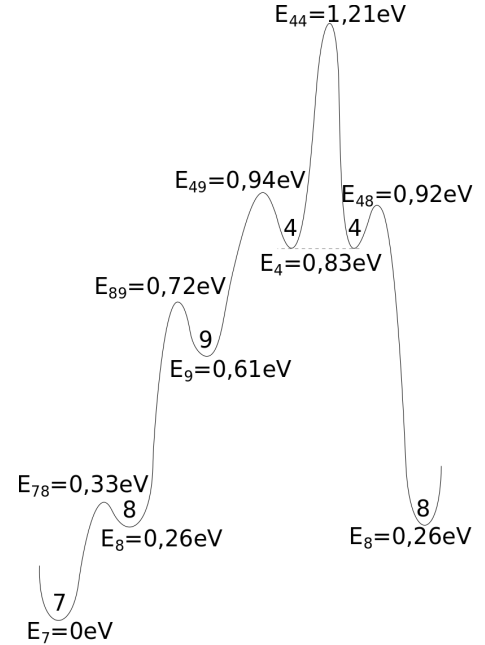


FIG. 2: Energy landscape cross-section along the marked path in Fig. 1. It contains all the possible Ga adatom jumps at the surface.

### III. DIFFUSION COEFFICIENT FOR Ga ADATOM AT GaAs(001) - $c(4 \times 4)\beta$ RECONSTRUCTION

Systematic study of energies of Ga atom at binding sites at GaAs(001) -  $c(4 \times 4)\beta$  surface reconstruction and of barriers for diffusion between them have been first shown in Ref 29. Lately more detailed map of the surface energy was presented in Ref. 1. We used the energy pattern calculated in this last article as a basis to the analysis of the diffusion behavior of adsorbed Ga atom.

The scheme of the lattice for Ga adsorption sites at GaAs(001) -  $c(4 \times 4)\beta$  surface is shown in Fig.1 with nu-

meration from Ref.1. When Ga atom was relaxed from  $3\text{\AA}$  above the surface seven different types of minimum energy sites were found. The lowest one with number 7 (described also as  $6^1$ ) lies in the trench between As dimers at the reconstructed surface and so are four other sites:  $8a, 8b$  and  $9a, 9b$ . As it was shown in Ref. 1 position and depth of the adsorption sites at hills of As dimers depends on the height from which Ga atom is relaxed. However if we stay at height of  $3\text{\AA}$  the surface is not deformed and there is only one additional adsorption site at the surface in two versions  $4a$  and  $4b$ . With the same numbers and different letters we marked sites of the same depth and the same jump rates out of the site, however with different space orientation, rotated or reflected like in the case of  $8a$  and  $8b$  (see Fig.1). All energies that decide about jump rates between our sites can be presented along path marked in Fig.1 and energy landscape along this path is shown in Fig.2. It can be seen that the site of the lowest energy is 7 and there are four different adsorption site energy values at this surface. All together there are seven sites - one of energy  $E_7$ , and two types of energies  $E_4, E_8$  and  $E_9$  in one elementary cage.

Calculated energy barriers determine the probability of each single particle jump. An analysis of barrier heights allows to find the easiest jump path, what have been done in Ref. 1. However when we look for the path with minimal energy barriers it does not necessarily reflect possible diffusional behavior of single particle. When particle moves randomly in the potential landscape like this in Figs. 1, 2 it jumps forward and backward with frequency proportional to the jump rate. As it can be seen when particle jumps down, into the site of lower energy, its return is more difficult due to high energy barrier. It means that not only transition rates of jumps but also site occupation probabilities at equilibrium should be also important in the long distance diffusive motion. Our formula (12) contains all transition rates as well as equilibrium occupation probabilities for all possible sites. Diffusion coefficient matrix describes long distance particle diffusion at equilibrium conditions. Below we calculate tensor of diffusion coefficients for single particle motion on using the variational approach. Then we compare diffusion in different directions and finally identify dominant diffusion paths. As we will see only some of them agree with the paths of minimal energy barriers.

In Fig.1 we plot all transitions between sites that are taken into account in the calculations below. Energy barriers for these transitions were taken from Ref.1. There is one more possible transition path not shown in Fig.1 but calculated in Ref.1. It is path directly from site 7 through low lying site 5 to the site 4 with the activation energy as high as  $1.10\text{eV}$ . In comparison with other energy barriers for jumps in the systems this transition rate can be neglected at experimentally achieved temperatures. As a result there is also no need to consider any additional sites, like 5, hence we end up with four different energies of adsorption sites.

According to the rules of statistical mechanics equilib-

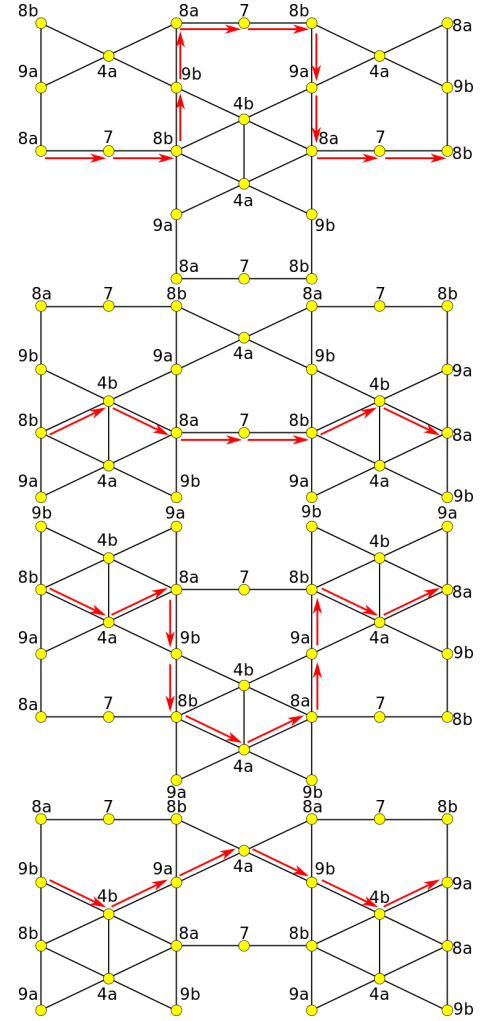


FIG. 3: Diffusion Ga adatom paths along the x-direction at GaAs(001)-c( $4 \times 4$ )  $\beta$  surface

rium probability at given site is

$$P_{eq}^{\alpha} = \frac{\rho e^{-\beta E_{\alpha}}}{2e^{-\beta E_4} + e^{-\beta E_7} + 2e^{-\beta E_8} + 2e^{-\beta E_9}} \quad (13)$$

when the site occupation is normalized within elementary cage  $\sum_{\alpha} P_{eq}^{\alpha} = \rho$ . Equilibrium probabilities (13) should be then put into the variational formula (12) for diffusion matrix. In general there are two variational parameters  $\phi_x^{\alpha}$  and  $\phi_y^{\alpha}$  per each site type - one coupled to the direction  $k_x$  and the other to  $k_y$ . The lattice has reflection symmetry with respect to the directions  $x$  and  $y$  and according to this symmetry  $\phi_{x,y}^{9a} = -\phi_{x,y}^{9b}$  - closest bonds are inverted in both directions, whereas  $\phi_x^{8a} = -\phi_x^{8b}$ ,  $\phi_y^{8a} = \phi_y^{8b}$  and inversely for the site 4,  $\phi_x^{4a} = \phi_x^{4b}$ ,  $\phi_y^{4a} = -\phi_y^{4b}$ . As mentioned before phases at one of sites can be set freely, so the number of parameters is reduced to six. Axes  $x$  and  $y$  are the main directions of the diffusional tensor  $\hat{D}$  for the lattice with the described symmetry, hence only diagonal parameters

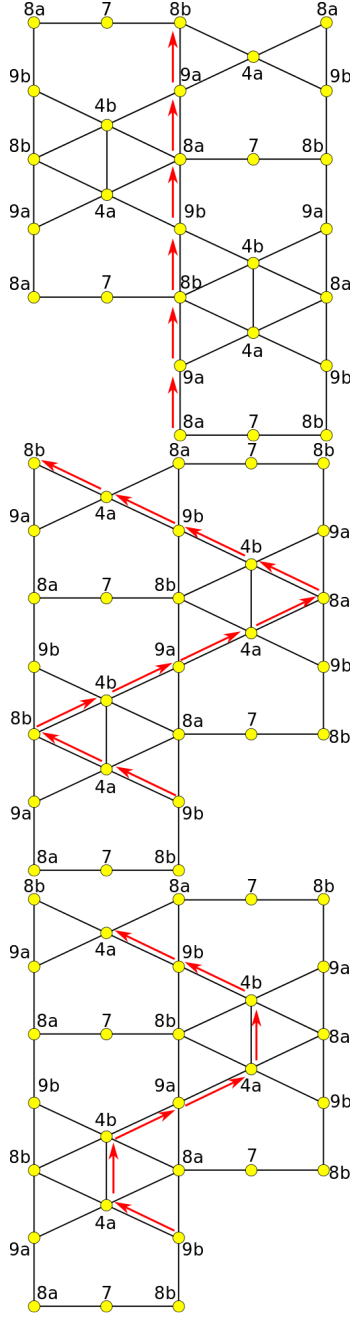


FIG. 4: Diffusion Ga adatom paths along the y-direction at GaAs(001)-c(4 × 4)β surface

$D_{xx} = D_x$  and  $D_{yy} = D_y$  are nonzero and each value at diagonal depends only on parameters coupled to the corresponding direction. Finally the following values of diffusion coefficients were found

$$D_x^\beta = 2 \left[ \frac{(W_{87}W_{89} + 4W_{84}W_{87} + 2W_{84}W_{89})P_{eq}^8}{2W_{84} + W_{87} + 2W_{89}} + W_{49}P_{eq}^4 \right] a^2 \quad (14)$$

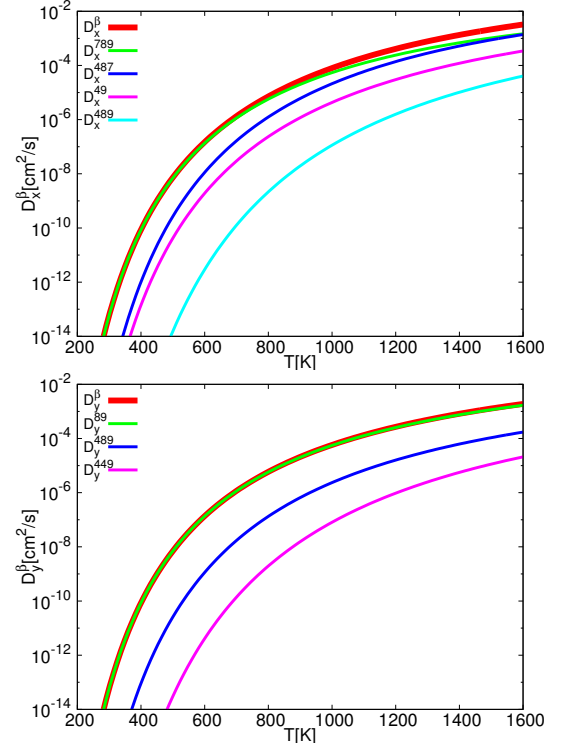


FIG. 5: Dependence of the diffusion coefficients  $D_x$  and  $D_y$  on the temperature for Ga atom at GaAs(001)-c(4 × 4) β surface

$$D_y^\beta = 2 \left[ W_{89}P_{eq}^8 + \frac{W_{49}(W_{44} + W_{48})P_{eq}^4}{W_{44} + W_{48} + W_{49}} \right] a^2 \quad (15)$$

where  $W_{\alpha,\beta}$  is given by Eq. (2) and appropriate energies can be found in Fig. 2. Lattice unitary length  $a = 5.6 \text{ \AA}$ .

In the above expressions each of terms can be understood as a contribution of a certain path to the total diffusion. Let us note that among all paths only one in direction  $x$  (between sites 4 and 9) and one in direction  $y$  (between sites 8 and 9) are independent from other ways of diffusion. Remaining transition rates of Eq. (14) and Eq.(15) are all connected in one component. The numerator of both these expression is a sum of separate terms. For example in Eq. (14) we can write first component as a sum of three terms, each of them containing two different rates in the numerator and the same rates in the denominator plus additional third one. Thus we can say that each of these terms represents path which goes through the main two links and it is slightly modified by the presence of other ways of diffusion. We can now plot all possible ways of diffusion. There are four paths in  $x$ -direction and three paths in  $y$ -direction. We show them in Figs 3 and 4.

At first let us analyze diffusion along direction  $x$ . The first plotted path contains only  $W_{87}$  and  $W_{89}$  transition rates and it is the same path as was identified as the one with the lowest activation energies for jumps in Ref. 1. In Fig.5 we plotted temperature dependence of total diffusion coefficient in both directions and contribution to

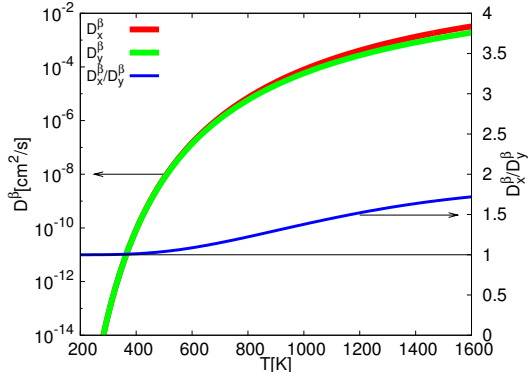


FIG. 6: Comparison of the diffusion coefficients  $D_x^\beta$  and  $D_y^\beta$  as a temperature function in logarithmic scale. The scale of the anisotropy coefficient is shown on the right.

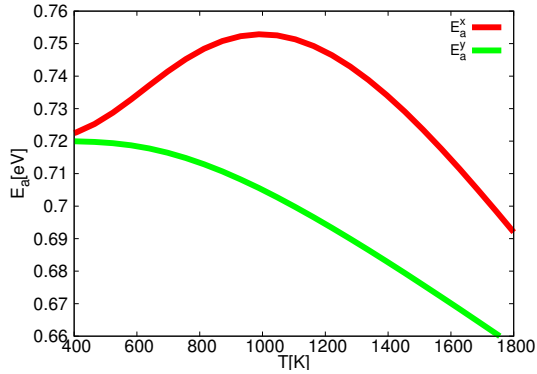


FIG. 7: Temperature dependence of the activation energies calculated with use of (18) for total diffusion coefficients  $D^\beta$  in both directions.

this value of each identified path. Our results confirm that path found in Ref. 1 is the most important for large temperature range. The next important path for the diffusion coefficient is the one that goes through the hill site 4. Diffusion along this path becomes larger than the first one at higher temperatures. As explained above these paths are not entirely independent, they are linked by denominator in one expression. This expression contains also third path, which has the lowest diffusion values. The independent path (49) is not the fastest one, but it is interesting because it bypasses site 7, the one of the lowest energy, what means that once particle comes out of the lowest energy site it can slide over states with higher energy. Such independent path and avoiding site 7 is the most important one in direction y. It appears that due to the symmetry of the lattice all possible paths along direction y bypass the lowest site as can be seen in Fig. 4. However according to plots in Fig. 5 only one path has significant effect on the overall diffusion in direction y.

It is interesting to compare diffusion along x and y direction. Components in both directions are plotted in Fig 6. It can be seen that diffusion in x direction is faster than

that in direction y. Note that this difference seems to be small only due to the logarithmic scale used in this figure. At the same figure ratio between  $D_x$  and  $D_y$  is plotted in linear scale. For low temperatures ratio between both diffusion components is close to one, i.e. in figure it is close to thin horizontal line of height 1. This agrees with Monte Carlo simulations in Ref. 29 where diffusion at temperature 470K was found to be isotropic. However at higher temperatures diffusion becomes an anisotropic process with  $D_x$  almost two times higher than  $D_y$ .

When we ignore in (14) and (15) all contributions from sites located at dipole structure we have expressions

$$\begin{aligned} D_x &= 2 \frac{W_{87}W_{89}P_{eq}^8}{W_{87} + 2W_{89}} a^2 \\ D_y &= 2W_{89}P_{eq}^8 a^2 \end{aligned} \quad (16)$$

which can be explicitly used to reproduce Monte Carlo (MC) data from (29). When we put into the above formulas exact energy barriers that were used in Ref. 29 we get  $D_x = 1.857 \cdot 10^{-8}$  and  $D_y = 1.859 \cdot 10^{-8}$  comparing with MC results  $1.74 \cdot 10^{-8}$  in direction x and  $1.66 \cdot 10^{-8}$  in direction y.

In order to analyze diffusion process more precisely we use parametrization

$$\begin{aligned} D_x &= \nu_x e^{-\beta E_A^x} \\ D_y &= \nu_y e^{-\beta E_A^y} \end{aligned} \quad (17)$$

where both activation energy  $E_A$  and prefactor  $\nu$  can weakly depend on temperature. We calculate activation energies on using the formula:

$$E_A = -\frac{\partial \ln D}{\partial \beta} \quad (18)$$

In Fig 7 we plot temperature dependence of activation energies for both coefficients  $D_x$ ,  $D_y$ . It can be seen that activation energy does not change much within the range of temperature which is important in the experiment. In both directions it starts with the same value 0.72 eV then  $E_A^x$  slightly goes up has its maximum at 1000K and then decreases, whereas  $E_A^y$  goes down within presented temperature range. It is interesting that even if  $D_y$  is lower than  $D_x$ , the effective activation energy responsible for this direction is also lower than  $E_A^x$ . It means that this is not activation energy but prefactor  $\nu$  that decides about the observed anisotropy. Looking at curves in Fig. 5 it is easy to understand that diffusion in the direction x is dictated by (789) direction at lower temperatures and then it is more and more dependent on the second channel (487), whereas diffusion along y direction is given almost totally by one, dominant component (89). The number of important diffusion paths contributes to prefactor, thus compensating the effect from the activation barrier difference.

We can see that at the surface with several adsorption sites and a complicated lattice of transitions few most important paths can be identified. In close to equilibrium



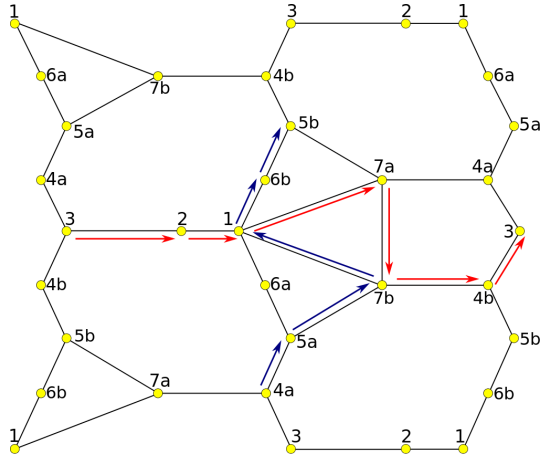


FIG. 8: Binding sites of Ga atoms at GaAs(001)-c(4 × 4) α surface.

conditions particles diffuse along these paths. We have shown that activation energy that characterizes given diffusion path is not a simple sum of energy barriers for individual jumps between successive adsorption sites. Equilibrium diffusion coefficient strongly depends on the occupation probabilities that always accompany corresponding transition rates. However the slowest jump in a row is the one that decides about the value of the diffusion coefficient. Such property can be seen in the shape of our formulas, where sums of the reciprocals of successive rates are present. Moreover diffusion process not necessarily happens through the lowest adsorption site, like our (89) path for diffusion along  $y$  direction.

#### IV. DIFFUSION COEFFICIENT FOR Ga ADATOM AT GaAs(001) - c(4 × 4)α RECONSTRUCTION

Let us take into regard c(4 × 4)α reconstruction of the same GaAs(001)surface<sup>2,24</sup>. The unit cell at this surface is similar one to this in the β reconstruction, but with slightly different position of atoms at top layer. As a result adsorption sites have completely different locations and energies<sup>2</sup>. Thus the symmetry of the energy landscape for Ga adatom is changed as can be seen in Fig 8. Note that we have now eleven different adsorption sites out of which nine (1,2,3,4a,4b,5a,5b,6a,6b) lie within trenches and two - namely 7a and 7b at dimer hills. The lattice has inverse symmetry only with respect to the axis  $x$ . There is no symmetry in the perpendicular direction. The cross-section of potential energy landscape along two paths marked in Fig. 8 is presented in Fig. 9.

Our calculations of diffusion coefficient start with formulas for equilibrium probabilities

$$P_{eq}^\alpha = \frac{\rho e^{-\beta E_\alpha}}{\sum_{i=1}^7 e^{-\beta E_i}} \quad (19)$$

Variational vector (11) is constructed with two indepen-

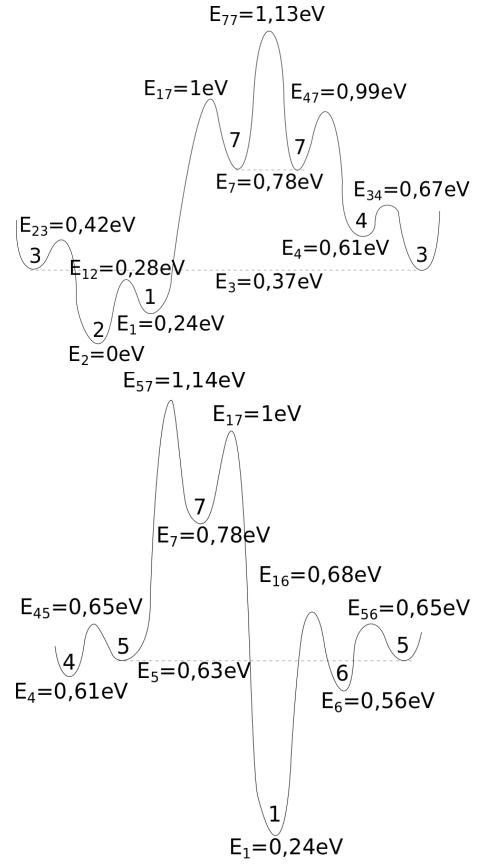


FIG. 9: Energy landscape along the marked paths in Fig. 8. They contain all the possible jumps of Ga adatom at the surface.

dent phases for each lattice site. According to the lattice symmetry  $\phi_y^3 = \phi_y^1 = 0$  and  $\phi_x^a = \phi_x^b$ ,  $\phi_y^a = -\phi_y^b$  for sites 4, 5, 6 and 7. Finally diffusion coefficients come out as

$$D_x^\alpha = \frac{W_{14}W'_{14}\theta_1 + W_{14}W'_{41}P_{eq}^4 + 2W'_{14}\tilde{W}_{41}\theta_4}{2W_{14} + W'_{14} + \tilde{W}_{14}}a^2 \quad (20)$$

$$D_y^\alpha = \frac{W_{14}W''_{14}P_{eq}^1P_{eq}^1 + W_{14}W_{43}P_{eq}^1P_{eq}^4}{W_{14}P_{eq}^1 + W''_{14}P_{eq}^1 + W_{43}P_{eq}^4}a^2 \quad (21)$$

where

$$\begin{aligned} \frac{1}{W_{14}P_{eq}^1} &= \frac{1}{W_{16}P_{eq}^1} + \frac{1}{W_{65}P_{eq}^6} + \frac{1}{W_{54}P_{eq}^5} \\ \frac{1}{W'_{14}P_{eq}^1} &= \frac{1}{2W_{17}P_{eq}^1 + 2W_{57}P_{eq}^5} + \frac{1}{2W_{74}P_{eq}^7} \\ \frac{1}{\tilde{W}_{14}P_{eq}^1} &= \frac{1}{2W_{43}P_{eq}^4} + \frac{1}{W_{32}P_{eq}^3} + \frac{1}{W_{21}P_{eq}^2} \\ \frac{1}{W''_{14}P_{eq}^1} &= \frac{1}{W_{17}P_{eq}^1 + W_{57}P_{eq}^5 + 2W_{77}P_{eq}^7} + \frac{1}{W_{74}P_{eq}^7} \end{aligned} \quad (22)$$

In the above expression all particle transitions plotted in Fig. 8 were taken into account, but two of them, namely

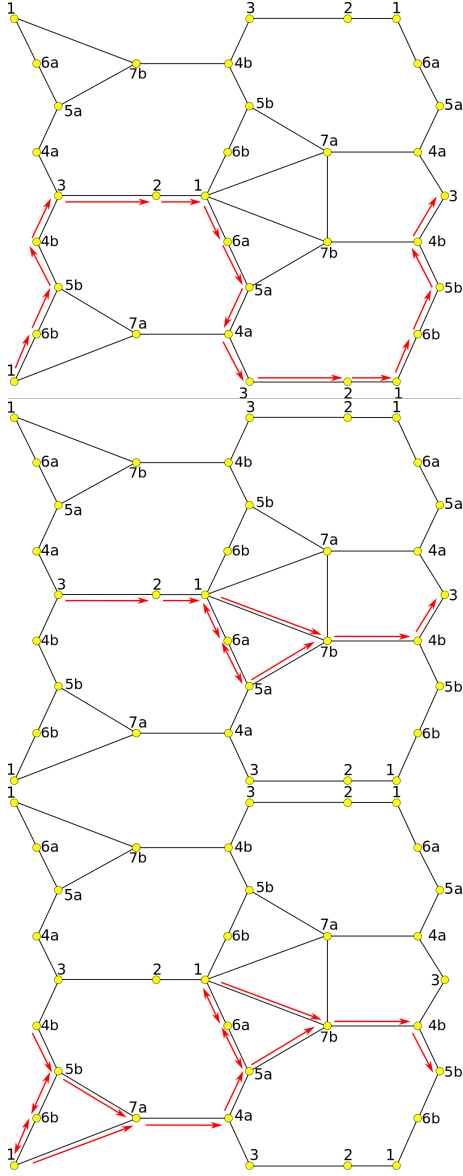


FIG. 10: Different Ga adatom diffusion paths in direction x over GaAs(001)  $(4 \times 4)\alpha$  reconstructed surface.

(57) and (17) were approximated by a simple sum as if they both come out from the site (1). This is an approximation of very fast jumps between (1) and (5), i.e. much faster than both jumps (57) and (17) what is true in our case. Formulas obtained with this approximation are not far from the exact solution, but they have simpler structure and give an opportunity to analyze different diffusion paths over the surface. These paths are plotted in Figs 10 and 11.

It can be seen that there are three possible ways over which particle diffuses in x direction and two in direction y. Their contributions to the global diffusion coefficient are presented in Figs 12 and 13. The fastest paths in both directions come along trench and do not climb the hill. Diffusion along axis x happens mainly through two

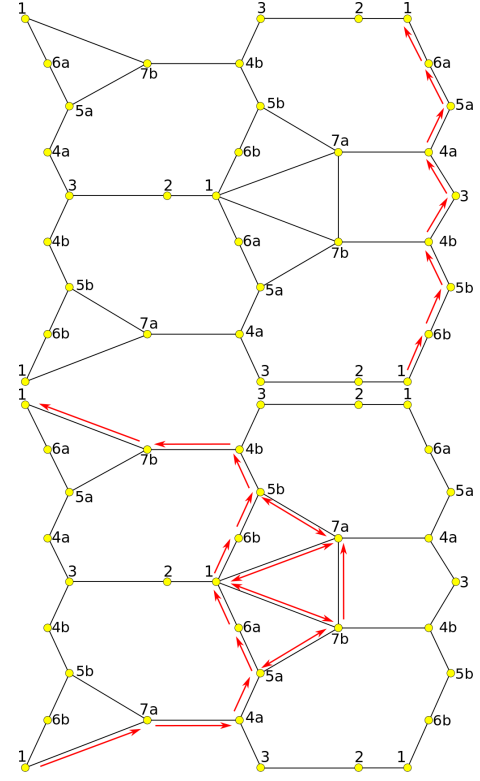


FIG. 11: Possible Ga adatom diffusion paths in direction y over GaAs(001)  $(4 \times 4)\alpha$  reconstructed surface.

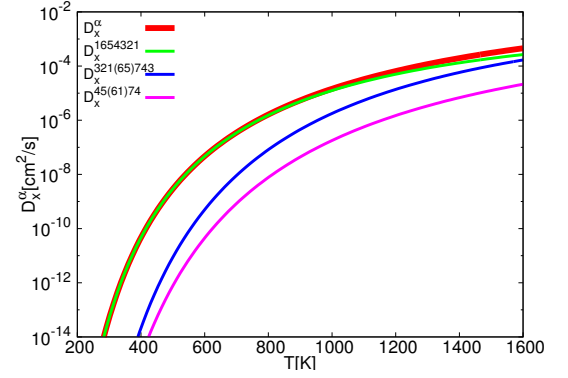


FIG. 12: Diffusion coefficient of Ga adatom in x direction over GaAs(001)  $(4 \times 4)\alpha$  reconstructed surface.

channels - first, more important one inside trench, and the second one visits also dimer hills. Both these channels were identified in Ref. 2 on the basis of energy differences for consecutive jumps. The fastest path in y direction comes through sites (16543) and covers almost totally the value of diffusion coefficient  $D_y$ . This last diffusion channel was not proposed before as a possible diffusion path<sup>2</sup> whereas it is important and interesting example of particle way that avoids the lowest energetically site (now it is site 2).

An anisotropy of the particle diffusion at the reconstructed surface  $(4 \times 4)\alpha$  is shown in Fig. 6. Within



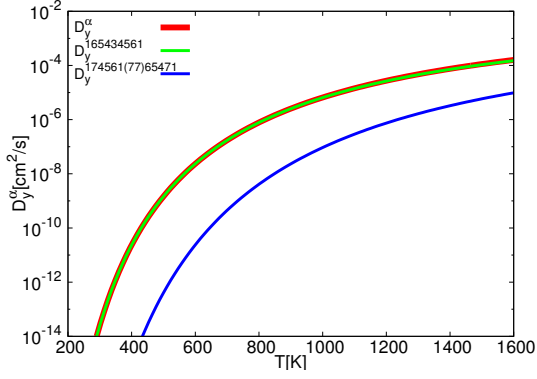


FIG. 13: Diffusion coefficient of Ga adatom in y direction over GaAs(001)  $(4 \times 4)\alpha$  reconstructed surface.

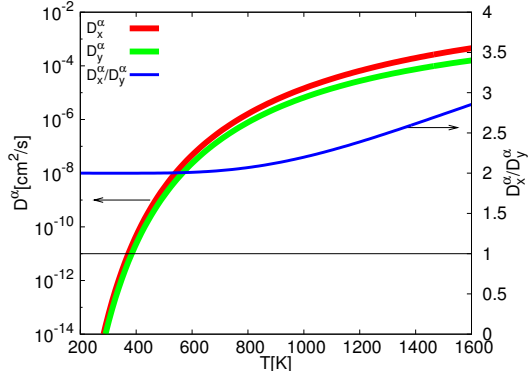


FIG. 14: Comparison of diffusion coefficients in x and y directions for GaAs(001)  $(4 \times 4)\alpha$  reconstructed surface as a temperature function in logarithmic scale. The scale of the anisotropy coefficient is shown on the right.

whole plotted range of temperatures diffusion is larger in direction x (parallel to dimers) than in direction y (perpendicular to dimers). Blue dashed line shows ratio between  $D_x$  and  $D_y$  coefficients. It starts from 2 at low temperature and increases to 3 for high temperatures. Thus comparing these values with those calculated for the surface  $(4 \times 4)\beta$  in Fig. 6 we conclude that the diffusion anisotropy is higher at  $\alpha$  surface reconstruction. It means that the change of surface symmetry affects symmetry of diffusion coefficient of single Ga particles. When we compare activation barriers for diffusion along direction  $x$  and  $y$  in Fig. 15 we find the same situation as at the previously described surface, namely  $E_A^x$  is larger than  $E_A^y$ . We again can explain this fact through the number of possible diffusion ways. Activation energies compared for diffusion over surface  $\alpha$  and  $\beta$  are lower for more complex structure of  $\alpha$  symmetry in both directions. We can understand such property as the dependence of the diffusion coefficient on larger number of transition rates in the  $\alpha$  phase. As a result overall diffusion coefficient has relatively low activation energy value and low prefactor  $\nu$ .

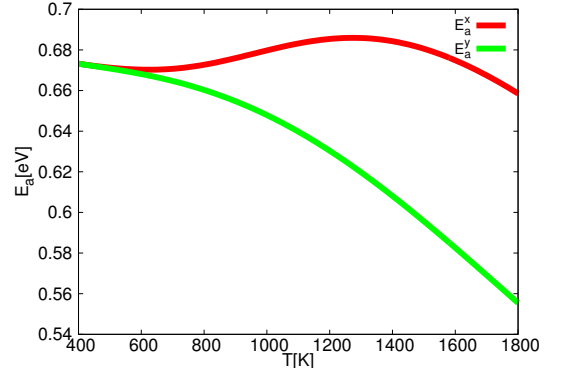


FIG. 15: Temperature dependence of the activation energies calculated with use of (18) for total diffusion coefficients  $D^\alpha$  in both directions.

## V. CONCLUSIONS

We have calculated diffusion coefficients for two versions of  $c(4 \times 4)$  reconstructed surface of GaAs(001)  $\beta$  and  $\alpha$  reconstructions. On using variational formula for the diffusion coefficient we were able to derive global expression for the elements of the diffusion coefficient tensor on the base of the derived in ab-initio calculations energy landscape of adsorption sites and energy barriers<sup>1,2</sup>. In the used here coordinate system our diffusion tensor has only diagonal elements. Diffusion along direction parallel to dimer orientation ( $x$ ) is higher in all cases. However at low temperatures at  $\beta$  surface phase diffusion is almost isotropic. The anisotropy increases with temperature and is higher for the  $\alpha$  surface phase.

The structure of diffusion coefficient as a sum of different components allows for identification of different diffusion paths. Some of these paths agree with ones guessed from the observation of energy barrier for successive jumps. The method allows for finding also other paths not so obvious while energy structure is studied. It appears that  $\alpha$  structure is far more asymmetric than  $\beta$  structure. And also when we compare values of coefficients it comes out that diffusion over the surface with lower symmetry,  $(4 \times 4)\alpha$  is of one order of magnitude lower than that for the surface of  $(4 \times 4)\beta$  symmetry. It appears that changes of surface structure towards system of lower symmetry can be noted in the decrease of the diffusion process. Faster, more effective diffusion process at given temperature is characteristic for the surface  $\beta$ , the reconstruction of higher symmetry.

## VI. ACKNOWLEDGEMENT

Research supported by the National Science Centre (NCN) of Poland (Grant NCN No. 2011/01/B/ST3/00526)

- 
- \* Electronic address: minkowski@ifpan.edu.pl, zalum@ifpan.edu.pl
- <sup>1</sup> J.L. Roehl, A. Kolagatla, V.K.K. Ganguri, S.V. Khare, R.J. Phaneuf, Phys. Rev. B **82**, 165335 (2010)
  - <sup>2</sup> J.L. Roehl, S. Aravelli, S. V. Khare, R. J. Phneuf, Surf. Sci. **606**, 1303 (2012)
  - <sup>3</sup> J.N Shapiro, A. Lin, D. L. Huffaker, and C. Ratsch, Phys. Rev. B **84**, 085322 (2011)
  - <sup>4</sup> W. D. Wheeler, B. A. Parkinson, and Y. Dahnovsky, J. Chem. Phys. **135**, 024702 (2011)
  - <sup>5</sup> J. Ferron, R. Miranda, and J. J. de Miguel Phys. Rev B **90**, 125437 (2014)
  - <sup>6</sup> Rafael Gonzalez-Hernandez, William Lpez-Prez, Mara Guadalupe Moreno-Armenta, and Jairo Arbey Rodriguez M J. Appl. Phys. **110**, 083712 (2011)
  - <sup>7</sup> S. Booyens, M. Bowker, and D. J. Willock, Surface Science **625** (2014) 6983,
  - <sup>8</sup> Yi-An Zhu, De Chen, Xing-Gui Zhou, P-O strand, and W-K Yuan, Surface Science **604** (2010) 186195
  - <sup>9</sup> A. Podsiady-Paszowska, M. Krawiec, Surface Science **622** (2014) 915,
  - <sup>10</sup> F. Liu, W. Hub, Y. Chen, H. Deng, H. Chena, X. Yang, W. Luod, Surface Science **624** (2014) 8994
  - <sup>11</sup> G. Antczak, G. Ehrlich, Surface Diffusion: Metals, Metal Atoms, and Clusters, Cambridge University Press, Cambridge, 2010.
  - <sup>12</sup> G. Antczak, Phys. Rev. B **73** (2006) 033406
  - <sup>13</sup> M. Krawiec and M. Jalochofski, Phys. Rev. B **87**, 075445 (2013)
  - <sup>14</sup> K.A. Fichthorn, Y. Tiwary, T. Hammerschmidt, P. Kratzer, M. Scheffler, Phys. Rev. B **83** (2011) 195328.
  - <sup>15</sup> A. Kley, P. Ruggerone, M. Scheffler, Phys. Rev. Lett. **79** (1997) 5278.
  - <sup>16</sup> A. Ohtake, Surf. Sci. Rep. **63** (2008) 295.
  - <sup>17</sup> V.H. Etgens, et al., Surf. Sci. **320** (1994) 252.
  - <sup>18</sup> U. Resch-Esser, et al., Surf. Sci. **352** (1996) 71.
  - <sup>19</sup> A. Nagashima, et al., Surf. Sci. **493** (2001) 227.
  - <sup>20</sup> T. Ito, K. Tsutsumida, K. Nakamura, Y. Kangawa, K. Shiraishi, A. Taguchi, and H. Kageshima, Applied Surface Science **237** (2004) 194199
  - <sup>21</sup> Shigeru Kaku, Jun Nakamura, Kazuma Yagyua, Junji Yoshino, Surface Science **625** (2014) 8489
  - <sup>22</sup> A. Nagashima, et al., Surf. Sci. **564** (2004) 218.
  - <sup>23</sup> E. Penev, et al., Phys. Rev. Lett. **93** (2004) 146102.
  - <sup>24</sup> A. Ohtake, J. Nakamura, Stsukamoto, N. Kogochi, A. Natori, Phys. Rev.Lett. **89**, 206102 (2002)
  - <sup>25</sup> M. Takahasi, J. Mizuki, Phys. Rev. Lett. **96** (2006) 055506.
  - <sup>26</sup> P. Jiřiček, et al., Surf. Sci. **603** (2009) 3088.
  - <sup>27</sup> A. Ohtake, et al., Surf. Sci. **566** (2004) 58.
  - <sup>28</sup> C.C. Matthai, G.A. Moran Applied Surface Science **123/124** (1998) 653-657
  - <sup>29</sup> J. G. LePage, M. Alouani, D. L. Dorsey, J. W. Wilkins, P. E. Blöchl, Phys. Rev. B **58**, 1499 (1998)
  - <sup>30</sup> M. Rosini, M. C. Righi, P. Kratzer, and R. Magri, Phys. Rev. B **79**, 075302 (2009)
  - <sup>31</sup> J. W. Haus and K. W. Kehr, Phys. Rep. **150**, 264 (1987)
  - <sup>32</sup> Z. W. Gortel, M. A. Załuska-Kotur, Phys. Rev. B **70** 125431 (2004)
  - <sup>33</sup> M.A. Załuska-Kotur, Z. W. Gortel, Phys. Rev. B **72** 235425 (2005)
  - <sup>34</sup> L. Badowski, M. A. Załuska-Kotur, Z. W. Gortel, Phys. Rev. B **72** 245413 (2005)
  - <sup>35</sup> M.A. Załuska-Kotur, Z. W. Gortel, Phys. Rev. B **74** 045405 (2006)
  - <sup>36</sup> L. Badowski, M. A. Załuska-Kotur, Z. W. Gortel, J. Stat. Mech. P03008 (2010)
  - <sup>37</sup> R. Gomer, Rep. Prog. Phys. **53**, 917 (2002).
  - <sup>38</sup> P. Pechukas, in Dynamics of Molecular Collisions: Part B, edited by W. H. Miller Plenum, New York, 1976.
  - <sup>39</sup> V. P LaBella, D. W. Bullock, C. Emery, Z. Ding and P. M, Thibado Appl.Phys. Lett. **79**, 3065 (2001)
  - <sup>40</sup> J. Schnakenberg, Reviews of Modern Physics, Vol. **48**, (1976), 571